"Out of sight, out of mind". The antagonistic role of the transcriptional memory associated with repeated acoustic stimuli on the priming of plant defense.

Khaoula Hadj-Amor[1,2,3],Ophélie Léger[2,3¶], Sylvain Raffaele[2¶], Magdalena Kovacic[1,3], Aroune Duclos[3,4], Pedro Carvalho-Silva[2], Frédérick Garcia[1,3,&*], Adelin Barbacci [2,3,&*]

1 Université de Toulouse, INRAE, Mathematiques et Informatique Appliquées de Toulouse (MIAT), 31326 Castanet-Tolosan, France.

2 Université de Toulouse, INRAE, CNRS, Laboratoire des Interactions Plantes Micro-organismes Environnement (LIPME), 31326 Castanet-Tolosan, France.

3 Interdisciplinary research group on the effect of mechanical VIbrations on Plants (VIP).

4 Laboratoire d'Acoustique de l'Université du Mans (LAUM), UMR 6613, Institut d'Acoustique - Graduate School (IA-GS), CNRS, Le Mans Université, Le Mans, France.

* corresponding authors

E-mail: frederick.garcia@inrae.fr, adelin.barbacci@inrae.fr

¶ These authors contributed equally to this work

& These authors also contributed equally to this work

Abstract (314 words)

Facilitating plant defense through priming holds significant promise for advancing sustainable crop health practices. The primed state of plants is correlated with a more rapid and efficient response, achievable by subjecting plants to recurrent stressors. Consequently, priming constitutes a dynamic transitional process between two distinct biological states, necessitating the establishment and maintenance of transcriptional memory mechanisms. Research on transcriptional memory has revealed molecular mechanisms including protein and transcription factor accumulation, as well as epigenetic modulations. Nonetheless, there remains a dearth of understanding regarding the interplay among the dynamics of transcriptional stress memory, its preservation, and the resultant emergent properties conferred upon the organism once primed. Here, we found that the robustness of transcriptional memory associated with repeated mechanical stimuli played an antagonistic role in the priming of plant defense. Incorporating experiments and computational modeling, we have analyzed the transcriptional stress memory of *Arabidopsis thaliana* subjected to daily acoustic stimulations. The observed enhanced resistance to the pathogen *Sclerotinia sclerotiorum* following three rounds of repeated acoustic stimulations is attributed to three primary mechanisms: the activation of a first line of defense in non-inoculated plants, an increase defense-associated gene diversification, and gene priming. These mechanisms are sustained by a transcriptional stress memory involving thousands of genes, likely regulated mostly by transcription factor cascades. Upon comparing the predictions of the transcriptional stress memory model with experimental outcomes, we propose that priming does not arise from the sequential activation of different pathways but rather from the simultaneous modulation of a broad spectrum of pathways. Pathway redundancy in the transcriptional memory topology imparts robustness to plant defense priming. Consequently, primed plants exhibit independence from limited genetic variations, preventing critical loss of resistance observed in naive plants. Pathway redundancies also imply strong

limitations in increasing plant defense. Thus, plants remain unaffected by an increase in the daily rate of RAS and exhibited a stress memorization time limited to 1.5 days.

Introduction

Like other living organisms, plants have evolved complex immune systems to restrict or halt the progression of pathogens. Plant immunity is commonly described as a interconnected layered system [1–3]. The initial layer involves the recognition by intracellular or surface molecular receptors of conserved patterns associated with pathogens. The perception of PAMPs by PRRs initiates a signaling cascade known as PTI. Pathogens have evolved effectors that can inhibit PTI but can also activate the second layer of the immune system, known as ETI. This form of resistance, particularly effective against biotrophic pathogens, operates on a key-lock model that, when triggered, confers complete immunity to the plant. However, minor variations in effector structure can enable the pathogen to circumvent the host system [2,4,5], and pathogens that thrive on dead plant cell may use plant programmed cell death to their benefit [6–8].

In the absence of qualitative resistance, a form of resistance known as quantitative resistance (QDR) is observed, which mitigates rather than halts disease progression [9,10]. This type of resistance is notable, for example, in response to necrotrophic fungi such as *Botrytis Cinerea* or *Sclerotinia sclerotiorum*. QDR is highly multigenic, involving the modulation of thousands of genes. Transcriptomic analysis of six species in the Pentapetalae family reveals that approximately 30% of transcriptomes respond locally to infection by the necrotrophic fungus *Sclerotinia sclerotiorum* [11]. Consequently, genes associated with quantitative disease resistance are not exclusively specific to the plant immune response. Polymorphisms in AtARPC4 regulatory region, a gene mediating actin filament reorganization, lead to enhanced resistance [12]. The high multigenicity of QDR is also influenced by abiotic stresses from the environment, such as temperature variations [13–15], and internal cues, such as mechanical fluctuations in cell walls [16] indirectly induced by necrotrophic fungi [17].

Plants exposed to recurring stresses may exhibit an enhanced response to subsequent stresses. These mechanisms, dependent on the plant's ability to memorize stress, enhance adaptation to its environment by accelerating and optimizing its response [18–20]. In the face of challenges in agriculture due to global warming, the imperative to reduce pesticide use, and the necessity to augment or sustain yields, harnessing plant priming mechanisms to design ideotypes presents a promising avenue for sustainable crop health management [20].

Plants can be conditioned to respond to a specific severe stress by initially subjecting them to a milder form of the same stress. For example, plant defense mechanisms can be activated by exposing plants to avirulent pathogens, conferring protection against secondary infections [21]. Stress exposure may also impart tolerance to unrelated stresses, as observed in wheat plants exposed to mild drought conditions, demonstrating increased resistance to low temperatures [22]. Plant priming is intricately associated with the plant's stress memory [23], influencing morphological, physiological, transcriptomic, and epigenetic dimensions.

Plant memory mechanisms exhibit diversity and remain inadequately comprehended [24]. Rather than being constrained by a static definition, plant memory is elucidated within the framework of how a system acquires, stores, and retrieves information, thereby influencing its subsequent behavior. Within the realm of plant biology, a myriad of memory mechanisms manifests, each characterized by distinct typical durations.

On a temporal scale of hours, rudimentary memory mechanisms, exemplified by the homogalacturonan cycle linked to pressure fluctuations, appear to operate autonomously of genetic influences [25,26]. Moving across temporal spans ranging from hours to generations, transcriptional memory emerges as the most viable candidate. To comprehend the modulation of gene expression influenced by a plant's memory of stresses, the primary focus lies in the investigation of epigenetic regulation and transcription factors [27]. As an instance, tri-methylation of histone H3 at lysine 4 and 9 (H3K4, H3K9) constitutes notable epigenetic modifications associated with the acclimation of poplar trees to recurrent mechanical stimuli. A singular bending event is demonstrated to be adequate to induce significant alterations in the overall abundance of these epigenetic marks [28]. Transcription factors, functioning as regulators of gene expression and mediators within signaling pathways, play also a crucial role in the intricate process of transcriptional memory, operating in synergy with epigenetic modifications. A case in point is FORGETTER3/HEAT SHOCK TRANSCRIPTION FACTOR A3 (FGT3/HSFA3), which is required for the establishment of physiological heat stress memory and the sustained maintenance of heightened memory-gene expression in the days following an exposure [29].

Recent studies provide robust evidence that sound induces molecular and physiological changes capable of enhancing plant resistance to disease [30–32]. Sound, characterized by minute temporal fluctuations in pressure, represents a form of mechanical stimulation. Nevertheless, the associated physical parameters present complexities in elucidating its perception by plants. For instance, a sound at 100 dB induces a pressure variation of 1 Pa, constituting a minuscule fraction of atmospheric pressure, and no mechanosensitive channel has been identified to respond to such low pressures [33], particularly at audible frequencies exceeding a few tens of hertz [34]. While the precise mechanisms underlying plant perception remain elusive, numerous impacts on plant function have been documented [35–38]. With regard to defense, a brief exposure of *Arabidopsis thaliana* plants to fixed-intensity sound vibrations modulates genes involved in response and signal transduction pathways. The genes affected depend on the frequency of the sound wave, but many involved in resistance, such as AtHSPRO2 (At2g40000), AtJAZ7 (At2g34600), and At5g66070, are modulated by most frequencies. Notably, phenotypic gains in resistance are reported only after repeated sound stimulation, indicating that *Arabidopsis thaliana* becomes more resistant to the necrotrophic fungus *Botrytis cinerea* after 10 days of sound treatment [30]. Transcriptomic and proteomic analyses reveal a profound effect of repeated acoustic stimulations (RAS) on reprogramming the plant's primary metabolism. However, the mechanisms through which transcriptional memory enables the plant to transition from a susceptible to a more resistant state remain unknown.

This study aims to dissect the interplay among the dynamics of transcriptional stress memory, its preservation, and the resultant emergent priming properties conferred upon *Arabidopsis* plants. We examined the modulation of RAS-induced plant resistance against the necrotrophic fungus *Sclerotinia sclerotiorum*. Our findings indicate that at least three RAS genes were necessary to achieve a 26% gain in resistance, independent of trichome density, which is putatively involved in sound perception. Transcriptomic analysis reveals that the resistance gain was correlated with the activation of primary defensive mechanisms in non-inoculated plants, including increased defense-associated genes diversification and gene priming. In-depth investigation into the transcriptional stress memory enhancing plant defense led to the development of a genome-scale quantitative model of the dynamic of gene regulations. Model analysis suggested that priming results from the parallel modulation of a broad spectrum of pathways rather than the sequential activation of pathways. *In silico* and experimental validations further confirmed that the RAS-mediated plant priming

mechanism was highly resilient, operating independently of limited genetic variations associated with resistance loss in naive plants. The robustness of priming, arising from the redundancy of gene regulatory mechanisms, also defined the limits of resistance enhancement in primed plants. Consequently, decreasing the interval between acoustic stimulations did not yield a corresponding increase in resistance. The predominance of gene regulation over modulation by the direct impact of acoustic stimuli resulted in a transcriptional memory persisting for only 1.5 days following cessation of stimuli.

Results

RAS-induced susceptibility decrease was independent of trichomes-mediated perception and required the repetition of stimulations.

To investigate the impact of repeated acoustic stimuli (RAS) on plant defense mechanisms, *Arabidopsis thaliana* genotypes at the four-week developmental stage were subjected to an escalating series of acoustic exposures prior to subsequent infection with the necrotrophic fungus *Sclerotinia sclerotiorum*. Each acoustic stimulus, characterized by 3 hours of 1000 Hz sinusoidal waves at 100dB (~1Pa), was administered every day for a variable duration spanning 1 to 10 days. The means by which plants perceive acoustic waves remain elusive, with a theoretical framework proposing trichomes on leaves and stems as potential acoustic wave sensors. According to this physical model, the slender morphology of trichomes could render them susceptible to bending induced by acoustic waves [39].

To ascertain the involvement of trichomes in the modulation of resistance under acoustic stimulation, we assessed resistance variations in various Arabidopsis mutants exhibiting natural alterations in shape and trichome density. The *arpc-4* mutant line, characterized by defects in actin polymerization and morphological changes in trichomes [12] and the gl-1 glabrous mutant line [40] were employed for this investigation. Following 10 repetitions of acoustic stimuli (AS), plant leaves were subsequently exposed to infection by the necrotrophic fungus *Sclerotinia sclerotiorum.* Plant susceptibility to infection was quantified by evaluating the growth rate of necrosis in leaves, as per the methodology outlined by Barbacci et al. [6].

Contrary to trichome-mediated perception, the reductions in susceptibility induced by RAS were found to be independent of genotype and trichome characteristics (Type II ANOVA, RAS: p-value = 2.79e-09, genotype: p-value = 9.98e-01, genotype x RAS: p-value = 9.54e-01). Notably, across all genotypes examined, exposure to 10 RAS consistently led to an approximate 20% reduction in susceptibility (**Fig. 1A**), irrespective of trichome morphology and density.

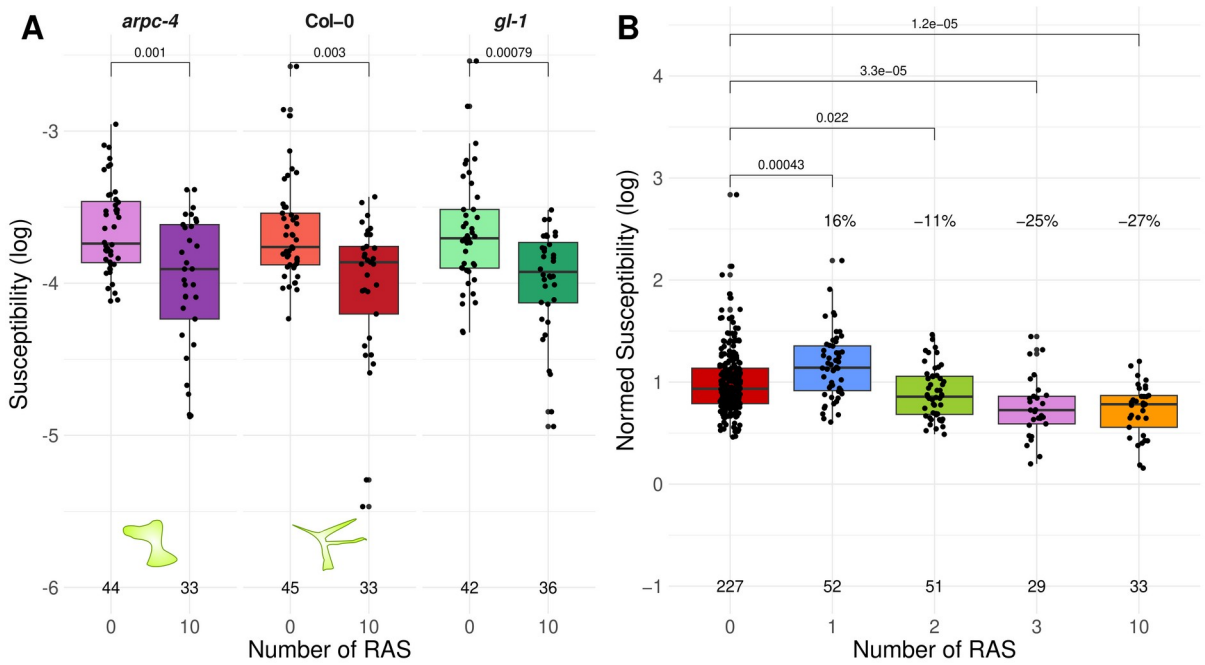

Figure 1. Impact of repeated acoustic stimulations (RAS) on plant susceptibility to *Sclerotinia sclerotiorum*. A. Approximately 25% reduction in susceptibility was observed with 3 hours of daily stimulation over a 10-day period, irrespective of genotypes affecting trichomes. **B.** The decline in susceptibility induced by repeated acoustic stimulation was established after three stimuli and maintained consistently. Boxplots indicate the interquartile range from the 25th to the 75th percentile, with the bold line representing the median. To enhance the granularity of information, jittered points are overlaid on the boxplot. Unpaired Welch's test p-values are indicated on the figure. The number of samples is indicated under each boxplot.

To further investigate the impact of the number of repeated acoustic stimuli (RAS) on the susceptibility of Col-0 *Arabidopsis* plants, varying quantities of RAS were administered prior to pathogen infection (**Fig. 1B)**. 2 RAS elicited approximately a 10% limited variation in susceptibility, maintaining levels closed from those observed in unstimulated plants. Beyond 3 RAS, a substantial gain in resistance of approximately 25% was conferred to the plants. Interestingly, the decrease in susceptibility induced by RAS remained constant beyond 3 repetitions, as plants subjected to 10 RAS exhibited a comparable reduction in susceptibility (**Fig. 1B**). Collectively, these findings suggested that the RAS-induced decrease in susceptibility was a dynamic process contingent upon the temporal integration of the plant's response to RAS, and notably, it appeared to be independent of the presence of trichomes.

RAS-associated transcriptional memory

To further understand the molecular basis underlying the progressive increase in plant resistance caused by repeated acoustic stimuli, we identified differentially expressed genes by RNA sequencing analysis in non-inoculated *Arabidopsis Col-0* plants exposed to RAS. RAS caused massive transcriptome reprogramming, and 35% of *A. thaliana* genes were modulated at least once by RAS. The modulated genes, as well as their number, varied considerably across RAS. Between 10% and 24% of the genome was modulated by RAS, with a minimum observed for 3 RAS (**Fig. 2A**). The limited number of genes expressed after 3 RAS may indicate RNA-decay mechanisms underpinning the phenotypic loss of susceptibility. Only 1422 (15%) of the 9554 RAS-modulated genes were expressed independently of the number of RAS, whereas 5578 (58%) were modulated by a specific number of RAS, showing a dominant transcriptional memory effect on gene expression (**Fig. 3**) and a clear memory discrimination between single stress and repeated stresses.

We compared these RAS-dependent transcriptomes with those of plants not exposed to RAS but infected with the necrotrophic fungus *S. sclerotiorum*. As previously reported [11], the *Arabidopsis* QDR to *S. sclerotiorum* is highly multigenic. Around 50% of *A. thaliana* genes were differentially expressed during infection (**Fig. 2B**). RAS conferred to non-inoculated plants a transcriptomic landscape partially similar to that of infected plants not exposed to acoustic waves. Transcriptome comparisons showed that RAS modulated up to 33% of QDR-associated genes in non-inoculated plants with a 14% minimum observed after 3 RAS (**Fig. 2B**). The genes were modulated by RAS in the same direction as during infection. The proportions remained stable when considering up- and down-regulated genes.

Ontology enrichment analysis [41] of RAS-modulated genes across the RAS showed that transcriptional memory did not result from the activation of mechanisms triggered after the first RAS only, but from the activation of parallel mechanisms over AS repetitions since biological processes and cellular components modulated in plants evolved progressively (**Fig. 2C,D**). The first acoustic stimulation led to the activation of response processes to different stimuli, abiotic stimulation probably downstream of acoustic stimulation perception, such as response to osmotic stress and endogenous stimulus (**Fig. 2C**). In parallel, the first RAS led to the activation of processes associated with plant-pathogen interactions, such as the response to chitin and the response to other organisms. RAS response genes participated to responses to different stresses or signals such as response to ethylene, light, hypoxia (**Sfile**). 3 RAS led to the modulation of other biological processes associated with responses to oxoacids such as oxalic acid secreted by *Sclerotinia sclerotiorum* [42] and the biosynthesis of carbohydrate structural elements (**Fig. 2C**). Consistent with the phenotypic analysis, 8 RAS led to the activation of a limited number of biological processes. Cellular component enrichment analysis [41] indicated that the RAS transcriptional memory was composed by key QDR physiological mechanisms (**Fig. 2D**). The first AS modulated Golgi and plasmodesmata involved in cell-cell junctions (**Fig. 2D**). The third AS caused changes in the endoplasmic reticulum and cell composition, whereas the eighth AS led to changes in the microtubules of the cytoskeleton (**Fig. 2D**).

Enrichment analyses suggested that mechanosensing and osmosensing were pathways involved in RAS-activated transcriptional memory. These signalling pathways are also involved in the regulation of the plant immune response. Mechanosensitive-like channels (AtMSL2, 3, 4, 6, 9 10) and MID1-complementing activity 1 (AtMCA1) are involved in jasmonic acid accumulation and lignin deposition [16]. Mechano-signalling triggered immunity (MTI), based on anisotropic cortical microtubule patterning, enhances plant

defence and contributes to 40% of the resistance phenotype [17]. Differential gene analysis confirmed the involvement of mechanosensing and osmosensing in transcriptional memory and RAS response. AtMSL5 and AtMSL10 were RAS-response genes modulated by the same amplitude after every RAS whereas MSL6 was involved in the transcriptional memory and modulated by 1 and 8 AS. AtMSL2, AtMSL3, AtMSL4, AtMCA1 were not modulated by RAS but only by infection. Regarding MTI, we identified 142 MTI-associated genes (**Sfile 1**) in the transcriptomic data set of this study. These genes, which were expressed during infection in the overstretched ring around the fungal colony in plants with regular cortical microtubule dynamics, also appeared to be modulated by RAS and involved in transcriptional memory and RAS response (**Fig. 2E**). 72% of MTI-associated genes were modulated after the first acoustic stimulation, 35% after 3 RAS and 60% after 8 RAS. 18% (25 genes) of the MTI-associated genes were response genes modulated independently of the number of RAS, while 8% were modulated in plants with increased resistance obtained after 3 RAS (**Fig. 1B**).

Epigenetic regulation and the collaborative action of transcription factors constitute pivotal elements shaping transcriptional memory [27,29,43]. To explore the potential implication of epigenetic regulators in RAS-induced transcriptional memory, we examined known epigenetic regulators associated with defense and thermal memory [20,44] in conjunction with our expression data. Out of the 31 epigenetic regulators identified in thermo-memory and defense, 10 exhibited RAS-depending expression in non-inoculated plants (**Fig. 2F**). To investigate the role of transcription factors (TFs) in the dynamics of RAS-induced transcriptional memory, we scrutinized TFs identified by motif analysis and provided by PlantTFDB [45] that were differentially expressed over RAS (**Fig. 2G, Sfile X**). TF expression was contingent upon the number of RAS exposures, with only 117 (20%) TFs being modulated independently of the repetition count. The expression of transcription factors (TFs) initiated a transcriptional cascade sustained by acoustic stimumation (AS), elucidating the progression of the observed transcriptomic landscape. Following the initial AS exposure, 176 TFs underwent modulation. This subset of highly interacting TFs subsequently governed the expression of 5227 (89% of 1 RAS DEGs) differentially expressed genes after a single stimulus and 80 differentially expressed TFs after three stimuli. Subsequently, TFs exhibiting differential expression after three repeated AS exposures regulated 1957 genes (74% of 3 RAS DEGs) and 163 TFs displaying differential expression after eight repeated AS exposures (**Fig. 2G**). This cascade of TF regulation over RAS suggested a mechanism supporting the kinematics of transcriptional memory (Fig. 2G), wherein TFs act as a repository of past states, enabling plants to discern the number of stimuli. All 18 TFs associated with MTI (Mechano-signaling Triggered Immunity) pathways were implicated in the TF transcription cascade, confirming the recruitment of MTI pathways in the transcriptional memory. These findings underscored that RAS initiated a transcriptional memory linked to the primed state of the plant. This memory, sustained at the molecular level, by transcription factors and epigenetic regulations, involved MTI and mechanoperception pathways.

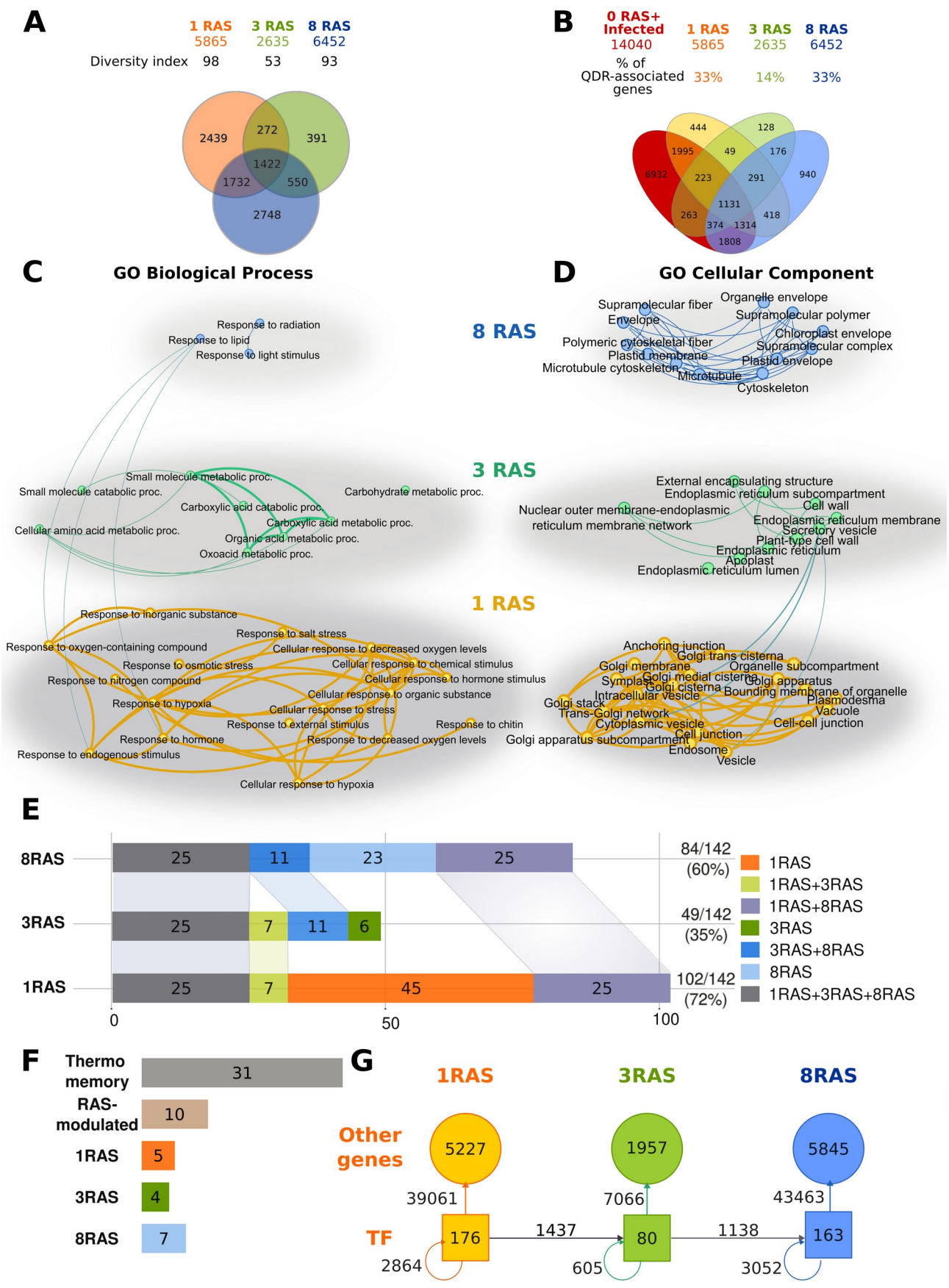

Figure 2. Impact of RAS on Gene Expression in non-inoculated **Plants. A**. Venn diagrams illustrating the genes expressed after 1, 3, and 8 RAS in non-inoculated plants. **B**. Venn diagrams representing genes expressed after 1, 3, and 8 RAS in non-inoculated plants compared to plants not subjected to RAS but infected by Sclerotinia sclerotiorum.

Numbers indicate the total count of differentially expressed genes. **C**. Enrichment analyses of biological processes ontologies during RAS. **D**. Enrichment analyses of cellular components ontologies during RAS. In panels C and D, a link between two nodes indicates that the two ontologies share more than 20% of genes. **E**. Differential expression of mechano-signaling-triggered immunity-associated genes over RAS. **F**. Number of thermo-memory and defense epigenetic regulator genes modulated by RAS. **G**. Transcription factor regulation cascade over RAS. Numbers in square boxes indicate the count of either transcription factors (TF) or other genes differentially expressed by RAS. Numbers over arrows indicate the number of regulations.

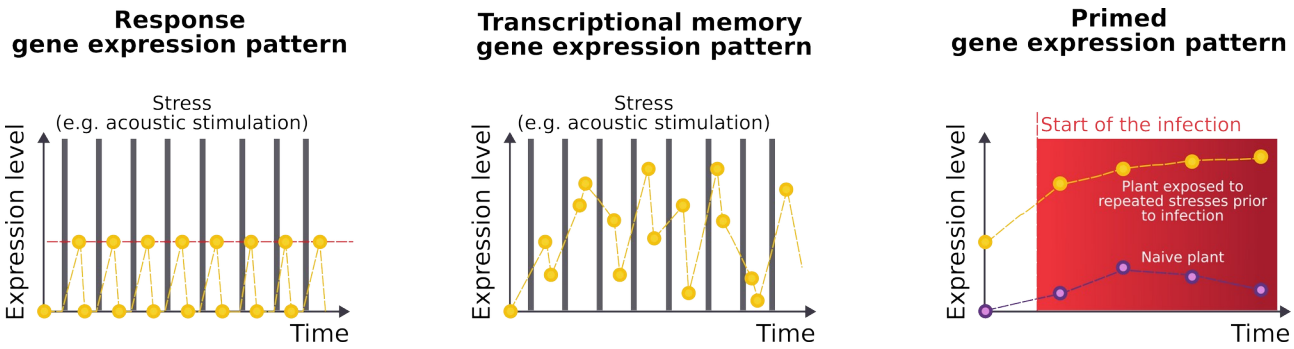

Figure 3. Gene expression patterns associated with repeated stresses. Response genes demonstrate consistent expression levels following each stimulation. The expression levels of transcriptional memory genes are contingent upon the prior history of stimulation. Primed genes exhibit a faster and higher expression level in plants that have been primed with stimuli before infection, as compared to naive plants that have not been exposed to such stimuli.

RAS triggered the recruitment of more QDR-associated genes and primed plant defense

Transcriptional memory is a fundamental mechanism in plant adaptation to fluctuating environments. To explore the molecular link between RAS transcriptional memory and plant QDR priming, we compared the transcriptomes of naive plants with those of RAS-exposed plants before infection by *S. sclerotiorum*. 4-week-old Arabidopsis Col-0 plants were exposed to RAS from 0 to 8 times. After the last acoustic stimulation, the plants were inoculated with the necrotrophic fungus *Sclerotinia sclerotiorum*. 24 h post-inoculation, cells at the periphery of the infection were harvested for RNA sequencing. The differentially expressed genes were identified by comparing gene expression in RAS-exposed and subsequently infected plants with non-inoculated naive plants (**Fig. 4**).

As is often observed with sequential stresses, transcriptomes are dominated by the last stress experienced by the plant [46]. Here, 96% of the 14040 QDR-associated genes modulated during infection in naive plants were also modulated at least once in RAS-exposed plants (**Fig. 4A**). This proportion remained stable over RAS for both up-and down-regulated genes, although a slight decrease below 90% was observed after 3 RAS (**Fig. 4B**). Plants exposed to AS prior to infection showed transcriptomic variations in around 10% of the genes. To test whether these changes depended on the interaction between the transcriptional memory and the infection context, we compared transcriptomes of non-inoculated plants with AS to transcriptomes of infected plants with and without AS (**Fig. 4C**). Most of the genes expressed in plants exposed to AS prior to infection were modulated only in the context of infection. Around 1000 genes were modulated in plants stimulated before infection, regardless of the number of AS (**Fig. 4C**). These genes recruited to RAS-exposed plants to participate likely in QDR were transcriptional memory-dependent. Most of these genes were modulated according to the number of AS, whereas only 348 were modulated regardless of the number of AS (**Fig. 4D**).

Enrichment analysis confirmed that the recruited genes contributed to the biological processes and cellular component diversification of the response to infection (**Fig. 4E,F**). Biological processes activated in RAS-exposed plants evolved with the number of RAS and modulated processes involved in the defense response (**Fig. 4E**). After 3 RAS, infected plants showed a higher number of genes involved in the response to endogenous stimuli and in the defense response to bacteria. After 8 RAS, plants also showed a higher response to lipids and ROS (**Fig. 4E**). Similarly, successive RAS induced changes in more cellular components. After 3 RAS, infected plants showed differences in the proteasome complex, consistent with the lower number of genes modulated (**Fig. 4F**).

Successive RAS have led to the diversification of activated QDR pathways in plants. The transcriptional memory that underlies such diversification is also a core mechanism of gene priming. Primed genes are characterized by faster and stronger responses (**Fig. 3**). We identified priming-related genes in both QDR-associated genes and recruited genes. We considered priming-related genes as genes that are more intensively modulated in RAS-treated plants compared to naive plants in the context of infection and are associated with the gain of resistance. 399 priming-related genes were found to be more intensively modulated in 3 and 8 RAS-exposed plants compared to 1 RAS-exposed and naive plants. 22 recruited genes were putative priming-related genes. Two MTI-associated genes were also priming-associated. AtCYP707A1 (AT4G19230) is involved in the defense response to fungi, while AtGIG1 (AT3G57860) controls entry into the second meiotic division and is a positive regulator of plant defense.

These results showed that RAS-triggered transcriptional memory led to an enhancement of the immune response through two mechanisms: diversification of the response by recruiting genes and priming of plant QDR genes.

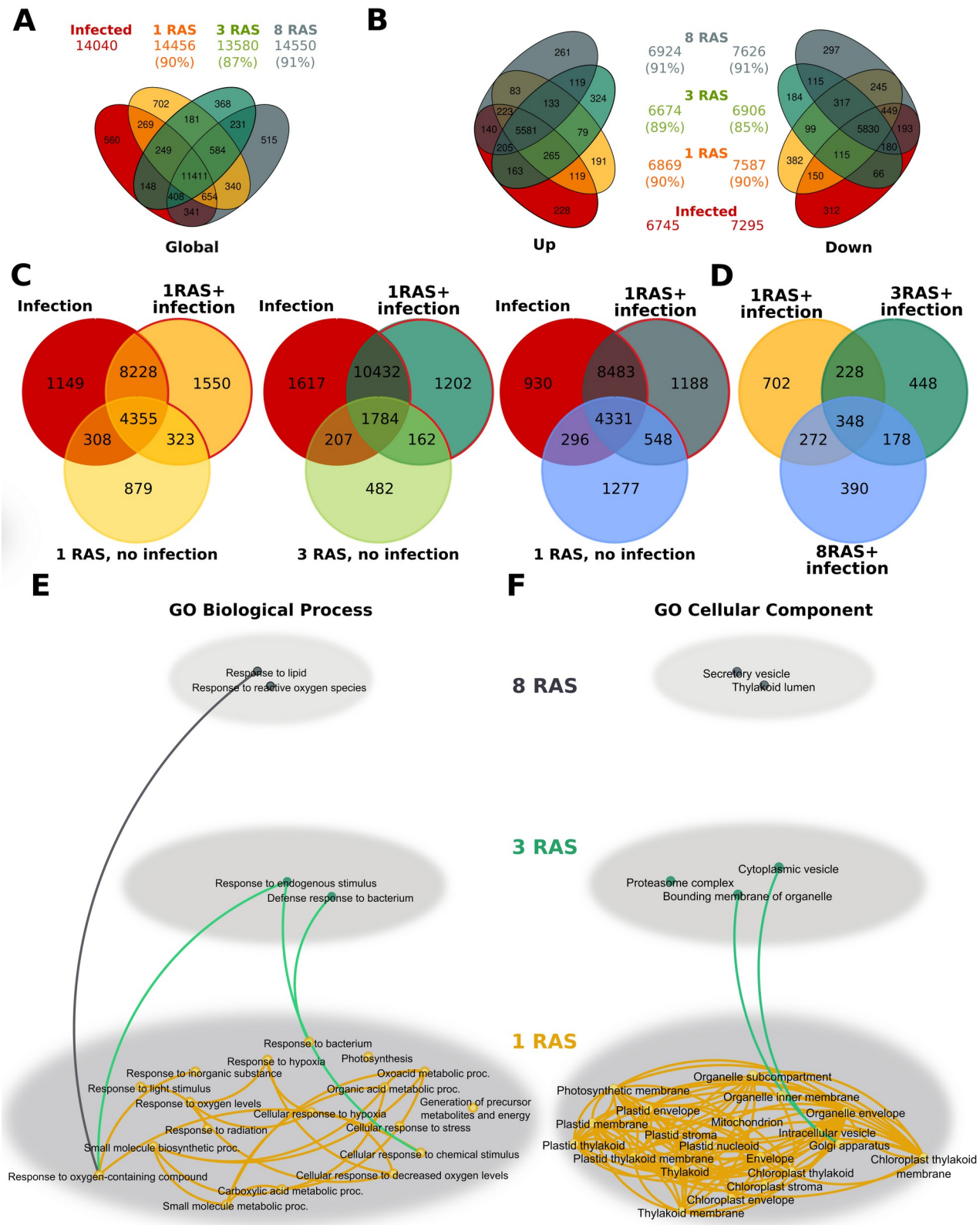

Figure 4. Impact of RAS on Gene Expression in Plants Exposed to RAS and Infected. A. Venn diagrams illustrating genes expressed after 1, 3, and 8 RAS in infected plants compared to the transcriptome of naive infected plants. **B**. Venn diagrams depicting up and downregulated genes. **C**. Venn diagrams showing genes expressed during infection, after RAS in non-inoculated and infected plants. **D**. Venn diagram highlighting genes expressed in RAS-exposed plants before infection, modulated only in the context of infection. **E**. Enrichment analyses of biological processes ontologies during RAS in infected plants. **F**. Enrichment analyses of cellular components ontologies during

RAS in infected plants. In panels E and F, a link between two nodes indicates that the two ontologies share more than 20% of genes.

Dynamic modeling of transcriptional memory and priming

To enhance our comprehension of the characteristics stemming from the transcriptional memory induced by repeated acoustic stimuli (RAS), we constructed a dynamic genome-scale gene network for non-inoculated plants exposed to RAS. Given the considerable number of genes in relation to the limited temporal description, we addressed this complexity by employing a clustering approach based on the sign of expression variation across RAS. This method, particularly suitable for very short time series, categorized genes into positive (+), negative (-), or null (=) variation between consecutive RAS. The cluster === that contained genes expressed at similar levels was excluded from further analysis. The resulting 26 clusters (**Fig. 5A**) exhibited diverse gene numbers, with distinct contributions from MTI-associated genes and transcription factors (TFs). Priming-associated genes, distributed across 50% of the clusters, contributed up to 9% to the overall cluster composition. Biological process enrichments (**Fig. 5A**) were observed in 15 clusters, reflecting modifications associated with RAS, including defense protein synthesis, structural alterations such as cell wall organization (cluster 6), and microtubule-dependent movements (clusters 4, 22), which are fundamental to MTI and plant defense.

To elucidate the temporal organization of plant responses to Repeated Acoustic Stimuli (RAS), we employed a modeling approach to capture gene expression patterns across both RAS occurrences and time. Assuming time-independent molecular regulations, we formulated gene expression as $dX/dt = A.X + B$, where dX/dt represents the temporal variation in the representative expression level of a gene cluster, X denotes the representative expression level of a gene cluster, A is a time-independent regulation matrix describing the regulation of all other gene clusters, and B is a fixed effect characterizing a constant RAS impact on gene expression. The resultant dynamic network consisted of 26 clusters interconnected by 184 oriented edges, unveiling a non-hierarchical organization with four distinct communities (**Fig. 5B**). These communities were characterized by a higher number of intra-community connections compared to inter-community connections. Notably, clusters associated with the perception of acoustic stimuli were distributed across 18 of the 26 clusters, underscoring the distributed nature of sound perception. Within the dynamic regulation network, three terminal nodes (12, 20, 24) were identified, each not implicated in the regulation of other genes (**Fig. 5A,B**). These nodes were associated with processes such as the response to chitin and endoplasmic stress (**Fig. 5A**). Given that the majority of clusters exhibited enhancements related to defense mechanisms, the responses linked to the terminal nodes were implemented as a complement to the other defense components deployed across the entire network.

To emphasize the dynamic implementation of transcriptional stress memory over RAS, we calculated the relative variation in gene expression between consecutive RAS (**Fig. 5C**). The first stimulation induced expression changes in nearly all clusters, with clusters 11 and 13 exhibiting particular susceptibility. Clusters 4, 11, and 16 served as regulatory proxies, integrating gene expression variations and governing numerous clusters. The third stimulation led to a reduction in gene expression in clusters 4 and 22, associated with microtubule-based processes, indicating a transition between the naive and primed states.

The modeling results suggest that the activation of RAS-associated transcriptional memory extends beyond so-called response genes, encompassing genes with complex expression profiles. This non-hierarchical and intricate organization facilitates the diversification of primed processes in plants exposed to RAS, underscoring the highly constrained nature of the plant immune response priming emerging from the transcriptional memory.

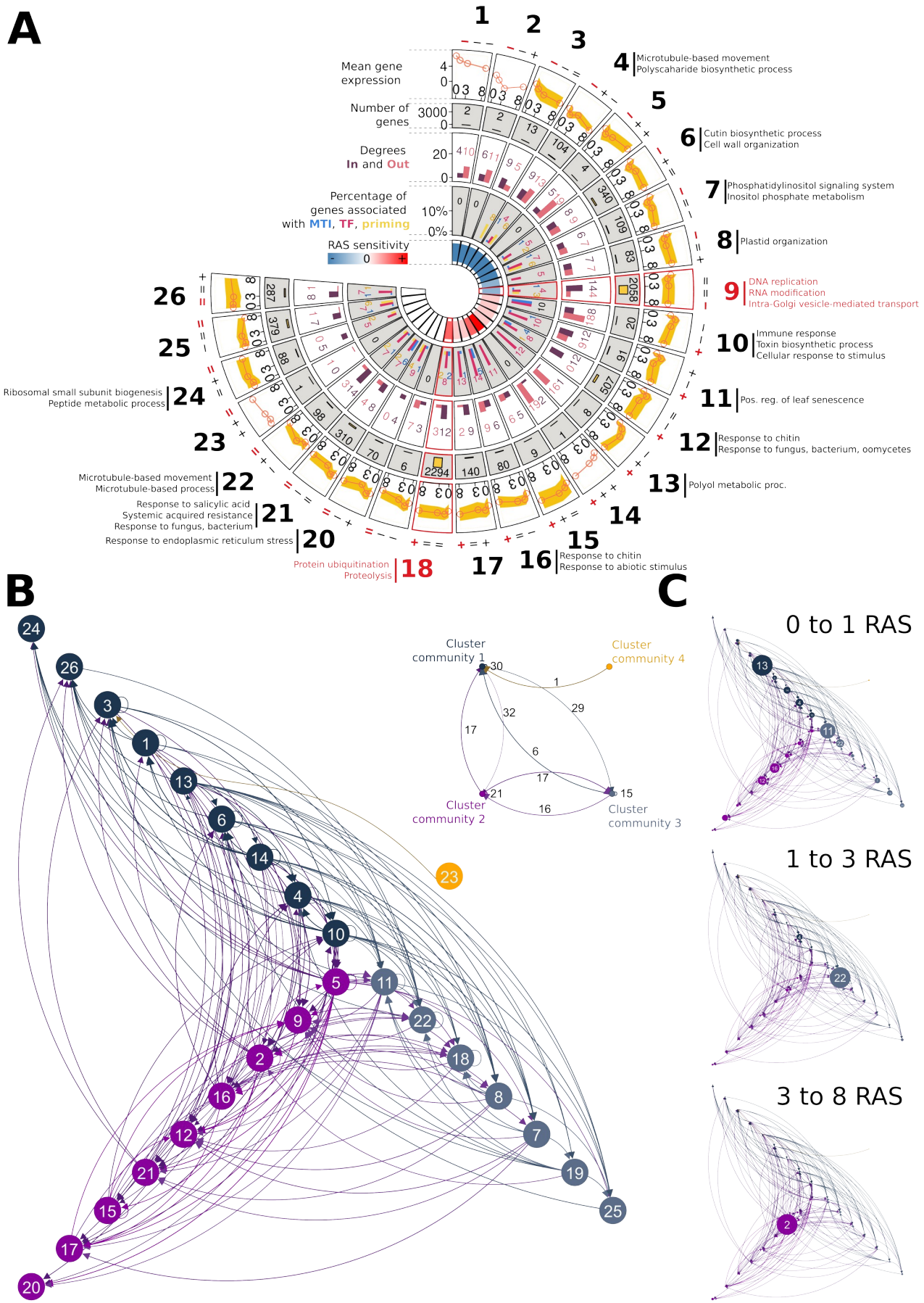

Figure 5. Dynamic Model of Plant Priming through Repeated Acoustic Stimulations (RAS). A. Characteristics of g clusters, their network connections, and the RAS-induced effect (B in the model) on gene expression. **B.** Dynamic

model of gene regulation (A matrix in the model) organized into four communities. **C.** Relative variations in gene expression during RAS.

Robustness of the priming of plant defense by RAS.

The robustness of plant immune response priming by Repeated Acoustic Stimulations (RAS) would be evident if it remained independent of specific gene clusters and variations in stimulation. To explore whether the robustness of plant defense priming by RAS is underpinned by the high connectivity of the network, we conducted *in-silico* experiments simulating gene deletions and assessed their impact on gene expression profiles and phenotypes. Initially, we performed an in-silico coarse knockout (KO) experiment, systematically varying each cluster's regulation in the A matrix by 1% and calculating the consecutive variation of the Root Mean Square Error (RMSE) induced in other clusters until the plant exhibited priming, i.e., after the third AS. The RMSE associated with the 1% regulation fluctuation was then compared to the RMSE obtained for the model accounting for all clusters (**Fig. 6A**). *In-silico* gene deletions resulted in RMSE variation of the same magnitude as the fluctuation (**Fig. 6A**), irrespective of the number of genes in the clusters. This suggests that immune response priming may be mostly associated with the synergistic response of all clusters rather than specific genes (Sfigure), implying that priming by RAS may be less dependent on most targeted deletions.

To experimentally corroborate these suggestions, we targeted plant mechanoperception pathways and monitored the variation of the resistance phenotype in primed and naive plants. We utilized the MSL quintuple mutant (msl4;msl5;msl6;msl9;msl10, denoted Δ5) and the mca1 mutant lines in the Col-0 background. Previous RNAseq data analyses indicated the involvement of MSL genes in transcriptional memory and plant priming by RAS. While MCA1 was not modulated by RAS, it exhibited differential expression during *S. sclerotiorum* infection. Mutant lines were exposed to three RAS sessions before infection by *S. sclerotiorum*. Phenotyping experiments revealed that naive mutant lines exhibited impaired resistance to the necrotrophic fungus, whereas primed plants exposed to RAS prior to infection displayed increased resistance after three RAS sessions (**Fig. 6B**).

To assess the effect of stimulus variation on the system, we simulated how the number of daily stimuli modulated gene expression. The simulation indicated that increasing the number of acoustic stimulations per day had minimal effects on representative cluster gene expression (**Fig. 6C**). However, when stimulations were spaced more than 1 day apart, greater variations in expression were observed, questioning the length of the memory window. To challenge the model's prediction regarding the minimal impact of an increased number of daily stimulations, we exposed Arabidopsis plants to two sessions of 3 hours of acoustic stimulation per day for 3 days before infection. Plants exposed to two stimuli per day remained less sensitive than native plants but slightly more susceptible than those exposed to only one stimulus per day (**Fig. 6D**).

These results demonstrate that priming by RAS restored the resistance phenotype of plants impaired in mechanoperceptive pathways. As suggested by the model, plant priming by RAS may involve intricate pathways acting synergistically. The high degree of interconnection between pathways contributed to robust priming mechanisms that are less dependent on targeted genetic variations. The question of the persistence of transcriptional memory was raised by the disruption of gene expression due to infrequent stimulation.

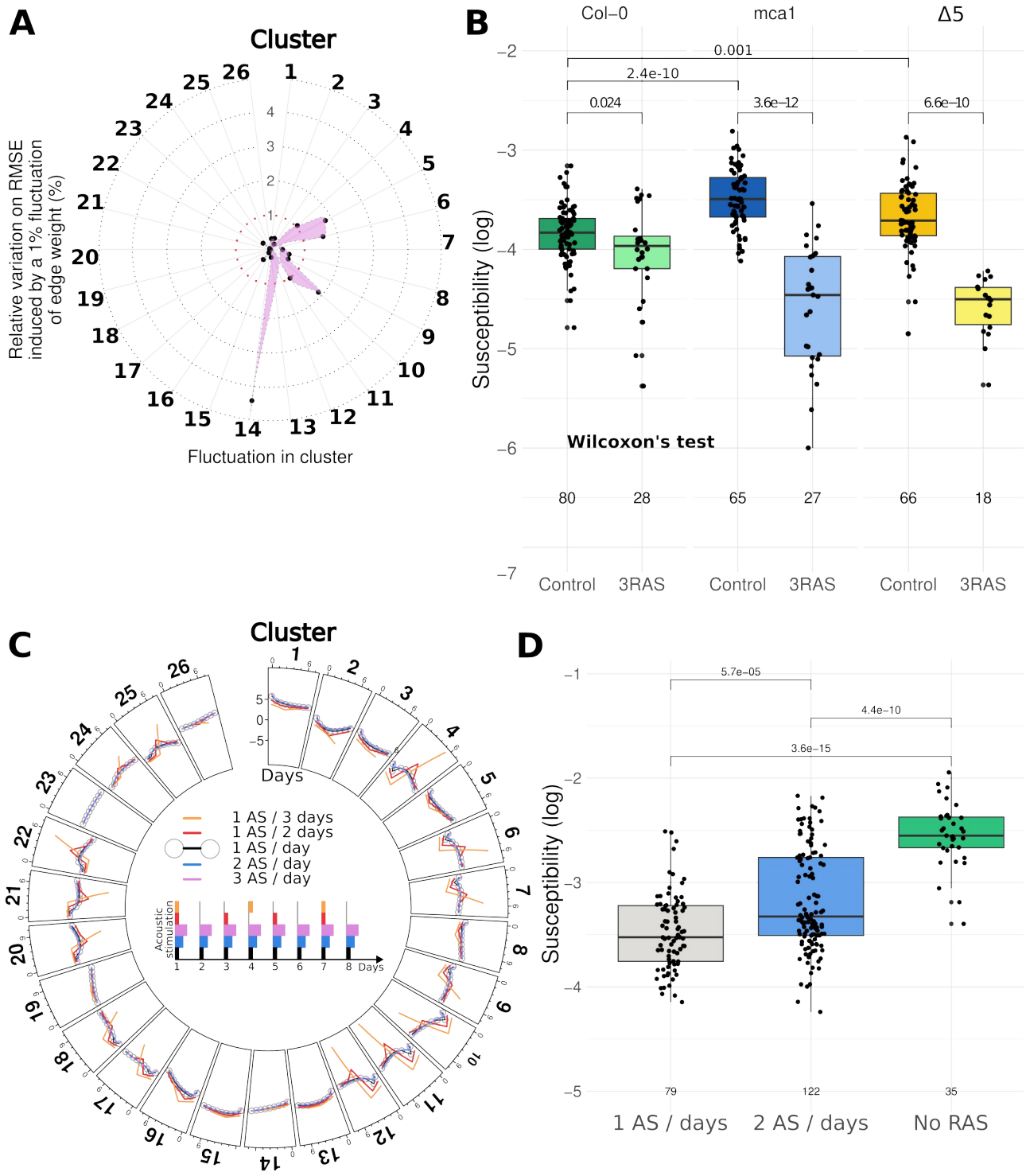

Figure 6. Robustness of the priming of plant defense by RAS. A. Simulation depicting the variation in gene expression Root Mean Square Error (RMSE) caused by a 1% fluctuation in gene regulation. **B.** Phenotypic variation in susceptibility between naive plants and plants exposed to Acoustic Stimulation (AS) three days prior to infection, illustrated for three different genotypes. **C.** Variations in gene expression associated with more and less frequent AS. Variation depicted over 8 days (external layer) with a description of the stimulation pattern (inner layer). **D.** Phenotypic variations in susceptibility to S. sclerotiorum for plants exposed to different RAS frequencies.

Length of window memory

The inquiry into the length of transcriptional memory arose from disruptions in gene expression following infrequent stimulation. To delve deeper into the temporal aspects of memory, we analyzed the eigen modes of the regulation matrix **A**. Each mode represents a linear combinations of clusters, elucidating how gene expression within clusters evolves in the absence of acoustic stimulation (AS). These modes were derived by computing the eigenvectors of matrix **A**, revealing that out of the 25 modes analyzed, 18 were stable modes characterized by eigenvalues possessing negative real parts. Conversely, the unstable modes had a limited impact on variations in gene expressions (**Fig. 8A**).

The first modes, contributing to >30% of the variation in gene expression, were all stable and embodied variations across 25 clusters over 26. Assessing the stability of these modes, the typical time for a mode to revert to its initial state was computed as the inverse of the real part of its eigenvalue (**Fig. 8B**). Consequently, the more a mode contributed to the total energy, the swifter it returned to its initial state. The overall system's typical time was calculated as the weighted time of the typical times associated with the first four stable modes.

Eigenvalue analysis suggested that a primed plant exposed to three Repeated Acoustic Stimulations (RAS) would lose its priming effect after 1.5 days without RAS. To validate this prediction, Col-0 plants were subjected to three RAS, and infections were initiated 0, 1, 2, and 3 days after the last stimulation (**Fig. 8C**). Phenotypic analysis revealed the persistence of the priming effect up to two days after the last stimulation, aligning with the model's prediction, but its efficacy waned after the third day without AS (**Fig. 8C**). This outcome underscored that the transcriptomic memory of *Arabidopsis* resistance primed by sound endured for less than three days.

Figure 7. Duration of the window memory. A. Contribution of every node to the total energy. Stable mode are in blue,

with the transcriptional memory of environmental stresses and antagonists of RNA decay (Crisp et al.). RNA decay is often linked to the establishment of a new functional biological regime (ref). Our transcriptomic data reveal though that the effective establishment of priming, occurring after 3 RAS, is accompanied by a robust RNA decay visible in both non-inoculated and primed plants before infection. Our simulations and experiments indicate that RAS memory persists simultaneously with RNA decay. Thus, RNA decay and epigenetic modifications may act synergistically to both maintain the memory of environmental stresses and ensure the plant's transition from a naive state to a primed state. The transmission of epigenetic marks to offspring is one of the biological mechanisms underlying the efficacy of priming methods in agriculture. We have demonstrated that after two days, primed plants no longer exhibit a resistance gain, suggesting that RAS priming is likely an effective technique for durations exceeding a few days. Similarly, the reversibility of the phenotype implies that structural modifications such as cell wall modifications associated with RAS are not decisive over 3 days for the increase in resistance gain in primed plants.

In our approach, we employed a dynamic gene regulation model without prior assumptions at the transcriptome level. The dynamic model proved effective in predicting key emerging phenotypic characteristics associated with transcriptional memory. Constructed at the genome scale, it successfully captured the intricacies of a multi-day phenomenon, offering a temporal resolution of one day. However, its applicability in describing the actual biological regulation between genes was limited. The identified relationships among clusters primarily held mathematical significance, hindering a comprehensive understanding of the biological underpinnings governing gene interactions. This limitation notably curtailed the exploration of genes upstream to transcriptional memory, particularly those implicated in transduction processes. A potential avenue for overcoming this constraint lies in adopting a similar mathematical approach but leveraging RNA-seq data with a more refined time step, characteristic of gene interactions. This nuanced approach could potentially unveil the early mechanisms underlying the perception of acoustic waves by plants, shedding light on the initiation of transcriptional memory. Research into the initial effects of acoustic waves on plants suggests that a more suitable time step for such investigations would be at the minute level, representing a temporal resolution approximately 1000 times finer than the data used in the current study. Adapting to this heightened temporal resolution could unravel previously unnoticed intricacies and provide a more detailed insight into the rapid responses and regulatory mechanisms triggered by acoustic stimuli in plant systems.

An increasing number of researchers propose that it is not implausible for the acoustic component of the ecological niche to inform the plant about its environment [36,37,47]. Apple and Cocroft [37] demonstrated that Arabidopsis thaliana plants exposed to vibrations caused by the chewing of the Pieris rapae caterpillar exhibited higher glucosinolate levels compared to plants subjected to vibrations from leafhoppers or wind. The findings of Apple and Cocroft suggest that the plant's response might be specific to the sound spectrum. In our study, the spectrum is limited to a peak at 1000 Hz. This frequency is more prominent in the spectrum of leafhoppers than in *Pieris rapae* ([37], Fig. 4a), yet it induces effective defense. The understanding of how plants perceive acoustic waves remains a barrier preventing a satisfactory interpretation of these experimental results.

Conclusion

In this study, we have investigated the effects of repeated acoustic stimulations on priming the plant's immune response. While the question of how plants perceive acoustic waves remains entirely open, the observed regulation of genes involved in the MTI (Mechano-signalling Triggered Immunity) by acoustic waves suggests the potentiation of plant mechanoperception as an integral part of defense priming through acoustic stimuli. This relationship, illustrated for the first time in this work, demonstrates the potential to gain a better understanding of the molecular aspects of thigmoimmunity, i.e., the regulation of plant immunity by mechanical forces [17].

Utilizing RNAseq, we have revealed the extent of molecular modifications associated with repeated acoustic stimulations, affecting approximately 25% of Arabidopsis thaliana genes. To comprehend this complexity, we inferred a dynamic genome-scale gene network. The gene network enabled us to elucidate how the robustness of genetic regulations constrains the phenotypic properties of the system. The established results, particularly the observed short duration of transcriptional memory window challenge the practical application of acoustic waves for crop health management in real agricultural practices. However, in this study, we opted to delineate the priming mechanisms induced by acoustic waves, which necessitate several days to manifest a phenotypic gain in resistance. Fine-tuning studies of gene expression dynamics before and after the initial stimulation may help isolate a more limited number of molecular actors, providing potential new avenues for controlling breeding selection.

Material & Methods

Plant / Fungal material cultivation and inoculation

Arabidopsis plants were cultivated under constant conditions, including a 9-hour light period at 120 µmol/m²/s, a temperature of 22°C, and a relative humidity of 70% for a duration of 4 weeks prior to inoculation and RNA sampling. The Sclerotinia sclerotiorum isolate (1980) was cultured on potato dextrose agar (PDA) plates at 25°C for 3 days before inoculation. Inoculation was carried out by placing a 5 mm diameter PDA plug on the adaxial surface of A. thaliana leaves, following the methodology described in Barbacci et al. [6]. Mock treatment involved using a S. sclerotiorum-free plug. For phenotypic assessments, infections were conducted on detached leaves within a humidity-controlled chamber, facilitating disease progression imaging [6]. RNA-seq analyses were performed on whole plants subjected to infections in the same chambers.

Phenotyping

Phenotyping was conducted on detached leaves within a controlled environment, characterized by elevated humidity and a constant temperature. The enclosed space, equipped with a camera, captured images at 10-minute intervals. Analysis of these images allowed for the measurement of lesion sizes on each leaf during infection. The susceptibility of individual leaves was subsequently calculated as the growth rate during the exponential phase of disease development, employing the segmented package in R [48]. Each phenotyping analysis presented in this paper was performed independently and repeated at least three times. For more information, please consult Barbacci et al. (2020). Python code for image analysis is available at https://github.com/darcyabjones/INFEST.

Sound priming and RNA sampling

After three weeks, the plants were transferred to two growth chambers under identical cultivation conditions. One growth chamber was equipped with a speaker (4” Visaton full range) connected to a power amplifier. The plants were subjected to acoustic stimulations during the initial three hours of the day (or the first six hours for two daily stimulations). The acoustic waves utilized were 1 kHz sinusoidal waves at a 100 dB intensity. Acoustic intensity was measured at the top of the plants using a sound intensity meter. Plants and leaves did not exhibit obvious variations of

phenotypes after RAS stimulation (plant or leaf size, colors ...). Infected plants were inoculated at the conclusion of the final stimulation session. Leaf samples were collected after the last acoustic stimulation for non-inoculated plants and 24 hours post-inoculation (hpi) for infected plants. Leaves were cut with a razor blade and immediately placed on a glass cooled by liquid nitrogen as in Sucher et al [11]. For every plants, a 2 mm thick ring around the infected area or the *S. sclerotiorum-free* plug (mock) was taken for RNA extraction.

RNA extraction and differential gene analysis

RNA extraction utilized the Nucleospin RNA kit from Macherey-Nagel. Subsequently, cDNA synthesis was carried out employing Superscript III reverse transcriptase (Invitrogen Carlsbad, CA) and 1 µg of total RNA. For RNAseq, reads were concurrently mapped against the genomes of A. thaliana Col-0 (TAIR10 release) and *S. sclerotiorum 1980*. This was accomplished using the nf-core/rnaseq pipeline version 3.0 [61], with specific parameters, namely "--skip_alignment --pseudo_aligner salmon." This set of parameters included adapter and quality trimming using Trim Galore software version 0.6.6, followed by transcript assignment and quantification using the salmon tool (version 1.4.0).

Differential gene analysis

Three differential gene expression analyses were conducted. To elucidate the impact of repeated acoustic stimulation (RAS) on gene expression in non-inoculated plants, we utilized the gene expression levels of uninfected plants that were not exposed to acoustic stimulation as the reference. Differentially expressed genes for non-inoculated plants exposed to 1, 3, and 8 RAS were then identified through three paired statistical tests based on the negative binomial distribution. Gene expression levels associated with Bonferroni-adjusted p-values below 0.05 were retained for further analysis. The same analytical process was employed to identify differentially expressed genes between consecutive RAS in non-inoculated plants and to understand the RAS effect on plants exposed to acoustic stimulation prior to infection. In the former case, the reference was the gene expression level of plants exposed to the previous RAS number. In the latter case, the reference was the gene expression level of plants not exposed to acoustic stimulation, considering infection as the reference. The analysis of differentially expressed genes was conducted using the R package DESeq2 [49].

Data analysis

Enrichment analysis and graphs were performed using ShinyGo [41]. MTI-associated genes were extracted from [17]. MTI-associated genes were genes differentially expressed in the overstretched ring around the necrosis in Col-0 compared to the impaired cortical mictorubules dynamics mutant line *pfd-6*. Transcription factors and transcription factors regulations were collected from the public database PlantTFDB [45] and are available in Sfile X. Statistics were computed using R software (ref). Test used is indicated in figure legend and in the main text. Plots were made with ggplot2 [50] and circlize [51] R libraries and combined with inkscape. Graphs were plotted using Gephi free software [52].

Clustering and dynamic gene network inference [KHA, FG]

The dataset details the expression profiles of approximately 9 954 genes differentially expressed across four distinct time points. The dimensions of the dataset initially posed a challenge for network inference. To address this, a crucial first step involved the substantial reduction of data dimensions using a clustering method. Traditional clustering approaches designed for static or dynamic data, such as k-means, were deemed unsuitable for our dynamic yet sparsely distributed temporal data. Consequently, a novel method was devised to categorize very short time series characterized by irregularly spaced time points. This method involved grouping genes with similar trajectories, and differential gene analysis was executed between consecutive time measurements to elucidate the temporal variations of each gene. Where expression significantly differed between two successive time points, the variations were designated as either positive (+) or negative (-). If the differences were not statistically significant, the temporal variation was denoted as zero (=).

Subsequently, genes were organized into 27 clusters based on similar expression signatures. Notably, the cluster representing genes with constant expression (===) was excluded from further analysis. The dynamic control network was derived through computation based on an extended explicit difference equation model, formulated as follows:

$$(X(t+dt)-X(t))/dt=A\cdot X(t)+B,$$

Here, $X(t+dt)$, $X(t)$, and B are vectors of length equal to the cluster number K, and A is a K×K square matrix. This equation represents the variation in the expression of a cluster-representative gene over time as a linear combination of the expression of cluster-representative genes of all clusters and a constant term B. The fixed effect of sound on cluster-representative gene expression is described by B. The model was constrained by the condition $AX(t=0)=0$, reflecting the fact that AS starts on day 1 (t=1). To ensure evenly spaced data over time, linear interpolation was applied between consecutive measurements when necessary. We assumed a univariate relationship among genes with similar order statistics within different clusters: genes exhibiting similar expressions in one cluster influence (and are influenced by) genes with similar expressions in other clusters. The A matrix and B vector were estimated using the LASSO estimator [53] implemented in the R package glmnet [54].

Acknowledgment

Khaoula Hadj-Amor's thesis is funded by INRAe's MathNumm department and the Occitanie region. AB and FG are funded by the templates project of the DIGITBIO metaprogram and the Thigmoimmunity project of the INRAe plant health department. SR was funded by the ERC VaryWheem. The authors would like to thank Jean-Marie Frachisse and Nathalie Leblanc-Fournier for seeds

References

1. Delplace F, Huard-Chauveau C, Dubiella U, Khafif M, Alvarez E, Langin G, et al. Robustness of plant quantitative disease resistance is provided by a decentralized immune network. Proc Natl Acad Sci U S A. 2020;117: 18099–18109. doi:10.1073/pnas.2000078117

2. Remick BC, Gaidt MM, Vance RE. Effector-Triggered Immunity. Annu Rev Immunol. 2023;41: 453–481. doi:10.1146/annurev-immunol-101721-031732

3. Roux F, Voisin D, Badet T, Balagué C, Barlet X, Huard-Chauveau C, et al. Resistance to phytopathogens e tutti quanti: Placing plant quantitative disease resistance on the map. Mol Plant Pathol. 2014;15: 427–432. doi:10.1111/mpp.12138

4. Derbyshire MC, Raffaele S. Surface frustration re-patterning underlies the structural landscape and evolvability of fungal orphan candidate effectors. Nat Commun. 2023;14: 5244. doi:10.1038/s41467-023-40949-9

5. Raffaele S, Kamoun S. Genome evolution in filamentous plant pathogens: why bigger can be better. Nat Rev Microbiol. 2012;10: 417–430. doi:10.1038/nrmicro2790

6. Barbacci A, Navaud O, Mbengue M, Barascud M, Godiard L, Khafif M, et al. Rapid identification of an Arabidopsis NLR gene as a candidate conferring susceptibility to Sclerotinia sclerotiorum using time-resolved automated phenotyping. Plant J. 2020; 1–15. doi:10.1111/tpj.14747

7. Derbyshire MC, Raffaele S. Till death do us pair: Co-evolution of plant–necrotroph interactions. Curr Opin Plant Biol. 2023;76: 102457. doi:10.1016/j.pbi.2023.102457

8. Govrin EM, Levine A. The hypersensitive response facilitates plant infection by the necrotrophic pathogen Botrytis cinerea. Curr Biol. 2000;10: 751–757. doi:10.1016/S0960-9822(00)00560-1

9. Poland JA, Balint-Kurti PJ, Wisser RJ, Pratt RC, Nelson RJ. Shades of gray: the world of quantitative disease resistance. Trends Plant Sci. 2009;14: 21–29. doi:10.1016/j.tplants.2008.10.006

10. Wang Z, Ma L-Y, Cao J, Li Y-L, Ding L-N, Zhu K-M, et al. Recent Advances in Mechanisms of Plant Defense to Sclerotinia sclerotiorum. Front Plant Sci. 2019;10: 1314. doi:10.3389/fpls.2019.01314

11. Sucher J, Mbengue M, Dresen A, Barascud M, Didelon M, Barbacci A, et al. Phylotranscriptomics of the Pentapetalae Reveals Frequent Regulatory Variation in Plant Local Responses to the Fungal Pathogen Sclerotinia sclerotiorum[OPEN]. Plant Cell. 2020;32: 1820–1844. doi:10.1105/tpc.19.00806

12. Badet T, Léger O, Barascud M, Voisin D, Sadon P, Vincent R, et al. Expression polymorphism at the ARPC4 locus links the actin cytoskeleton with quantitative disease resistance to Sclerotinia sclerotiorum in Arabidopsis thaliana. New Phytol. 2019;222: 480–496. doi:10.1111/nph.15580

13. Aoun N, Tauleigne L, Lonjon F, Deslandes L, Vailleau F, Roux F, et al. Quantitative disease resistance under elevated temperature: Genetic basis of new resistance mechanisms to ralstonia solanacearum. Front Plant Sci. 2017;8: 1–16. doi:10.3389/fpls.2017.01387

14. Didelon M, Khafif M, Godiard L, Barbacci A, Raffaele S. Patterns of Sequence and Expression Diversification Associate Members of the PADRE Gene Family With Response to Fungal Pathogens. Front Plant Sci. 2020;11: 1–16. doi:10.3389/fgene.2020.00491

15. Singh BK, Delgado-Baquerizo M, Egidi E, Guirado E, Leach JE, Liu H, et al. Climate change impacts on plant pathogens, food security and paths forward. Nat Rev Microbiol. 2023;21: 640–656. doi:10.1038/s41579-023-00900-7

16. Engelsdorf T, Gigli-Bisceglia N, Veerabagu M, McKenna JF, Vaahtera L, Augstein F, et al. The plant cell wall integrity maintenance and immune signaling systems cooperate to control stress responses in Arabidopsis thaliana. Sci Signal. 2018;11. doi:10.1126/scisignal.aao3070

17. Léger O, Garcia F, Khafif M, Carrere S, Leblanc-Fournier N, Duclos A, et al. Pathogen-derived mechanical cues potentiate the spatio-temporal implementation of plant defense. BMC Biol. 2022;20: 292. doi:10.1186/s12915-022-01495-w

18. Baier M, Bittner A, Prescher A, van Buer J. Preparing plants for improved cold tolerance by priming. Plant Cell Environ. 2019;42: 782–800. doi:10.1111/pce.13394

19. Conrath U. Molecular aspects of defence priming. Trends Plant Sci. 2011;16: 524–531. doi:10.1016/j.tplants.2011.06.004

20. Liu H, Able AJ, Able JA. Priming crops for the future: rewiring stress memory. Trends Plant Sci. 2022;27: 699–716. doi:10.1016/j.tplants.2021.11.015

21. Li JL, Wu FC, Zhu FX. Fitness is recovered with the decline of dimethachlon resistance in laboratoryinduced mutants of Sclerotinia sclerotiorum after long-term cold storage. Plant Pathol J. 2015;31: 305–309. doi:10.5423/PPJ.OA.04.2015.0066

22. Bruce TJA, Matthes MC, Napier JA, Pickett JA. Stressful “memories” of plants: Evidence and possible mechanisms. Plant Sci. 2007;173: 603–608. doi:10.1016/j.plantsci.2007.09.002

23. Crisp PA, Ganguly D, Eichten SR, Borevitz JO, Pogson BJ. Reconsidering plant memory: Intersections between stress recovery, RNA turnover, and epigenetics. Sci Adv. 2016;2: e1501340–e1501340. doi:10.1126/sciadv.1501340

24. Barbacci A, Lahaye M, Magnenet V. Another Brick in the Cell Wall: Biosynthesis Dependent Growth Model. PLoS ONE. 2013;8.

25. Proseus TE, Boyer JS. Calcium pectate chemistry causes growth to be stored in Chara corallina: A test of the pectate cycle. Plant Cell Environ. 2008;31: 1147–1155. doi:10.1111/j.1365-3040.2008.01829.x

26. Avramova Z. Defence-related priming and responses to recurring drought: Two manifestations of plant transcriptional memory mediated by the ABA and JA signalling pathways. Plant Cell Environ. 2019;42: 983–997. doi:10.1111/pce.13458

27. Ghosh R, Roué J, Franchel J, Paul A, Leblanc-Fournier N. Temporal modification of H3K9/14ac and H3K4me3 histone marks mediates mechano-responsive gene expression during the accommodation process in poplar. bioRxiv. 2023; 2023.02.12.526104. doi:10.1101/2023.02.12.526104

28. Friedrich T, Oberkofler V, Trindade I, Altmann S, Brzezinka K, Lämke J, et al. Heteromeric HSFA2/HSFA3 complexes drive transcriptional memory after heat stress in Arabidopsis. Nat Commun. 2021;12: 3426. doi:10.1038/s41467-021-23786-6

29. Choi B, Ghosh R, Gururani MA, Shanmugam G, Jeon J, Kim J, et al. Positive regulatory role of sound vibration treatment in Arabidopsis thaliana against Botrytis cinerea infection. Sci Rep. 2017;7: 2527. doi:10.1038/s41598-017-02556-9

30. Ghosh R, Gururani MA, Ponpandian LN, Mishra RC, Park S-C, Jeong M-J, et al. Expression Analysis of Sound Vibration-Regulated Genes by Touch Treatment in Arabidopsis. Front Plant Sci. 2017;8: 100. doi:10.3389/fpls.2017.00100

31. Ghosh R, Mishra RC, Choi B, Kwon YS, Bae DW, Park S-C, et al. Exposure to Sound Vibrations Lead to Transcriptomic, Proteomic and Hormonal Changes in Arabidopsis. Sci Rep. 2016;6: 33370. doi:10.1038/srep33370

32. Liu SB, Jiao JJ. Arabidopsis Leaf Trichomes as Acoustic Antennae. Biophysj. 2017;113: 1–5. doi:10.1016/j.bpj.2017.07.035

33. Chehab EW, Yao C, Henderson Z, Kim S, Braam J. Arabidopsis touch-induced morphogenesis is jasmonate mediated and protects against pests. Curr Biol. 2012;22: 701–706. doi:10.1016/j.cub.2012.02.061

34. Ge SX, Jung D, Yao R. ShinyGO: a graphical gene-set enrichment tool for animals and plants. Bioinformatics. 2020;36: 2628–2629. doi:10.1093/bioinformatics/btz931

35. Cessna SG, Sears VE, Dickman MB, Low PS. Oxalic acid, a pathogenicity factor for Sclerotinia sclerotiorum, suppresses the oxidative burst of the host plant. Plant Cell. 2000;12: 2191–2199. doi:10.1105/tpc.12.11.2191

36. Hilker M, Schmülling T. Stress priming, memory, and signalling in plants. Plant Cell Environ. 2019;42: 753–761. doi:10.1111/pce.13526

37. Ding B, Wang G-L. Chromatin versus pathogens: the function of epigenetics in plant immunity. Front Plant Sci. 2015;6. Available: https://www.frontiersin.org/articles/10.3389/fpls.2015.00675

38. Jin J, Tian F, Yang D-C, Meng Y-Q, Kong L, Luo J, et al. PlantTFDB 4.0: toward a central hub for transcription factors and regulatory interactions in plants. Nucleic Acids Res. 2017;45: D1040–D1045. doi:10.1093/nar/gkw982

39. Desaint H, Aoun N, Deslandes L, Vailleau F, Roux F, Berthomé R. Fight hard or die trying: when plants face pathogens under heat stress. New Phytol. 2021;229: 712–734. doi:10.1111/nph.16965

40. Muggeo VMR. Estimating regression models with unknown break-points. Stat Med. 2003;22: 3055–3071. doi:10.1002/sim.1545

41. Love MI, Huber W, Anders S. Moderated estimation of fold change and dispersion for RNA-seq data with DESeq2. Genome Biol. 2014;15: 550. doi:10.1186/s13059-014-0550-8

42. Wickham H. Ggplot2. 2009; 9–27. doi:10.1007/978-0-387-98141-3

43. Gu Z, Gu L, Eils R, Schlesner M, Brors B. circlize implements and enhances circular visualization in R. Bioinformatics. 2014;30: 2811–2812. doi:10.1093/bioinformatics/btu393

44. Bastian M, Heymann S, Jacomy M. Gephi: An Open Source Software for Exploring and Manipulating Networks. Proc Int AAAI Conf Web Soc Media. 2009;3: 361–362. doi:10.1609/icwsm.v3i1.13937

45. Tibshirani R. Regression Shrinkage and Selection Via the Lasso. J R Stat Soc Ser B Methodol. 1996;58: 267–288. doi:10.1111/j.2517-6161.1996.tb02080.x

46. Friedman JH, Hastie T, Tibshirani R. Regularization Paths for Generalized Linear Models via Coordinate Descent. J Stat Softw. 2010;33: 1–22. doi:10.18637/jss.v033.i01